Published in final edited form as:
Biomaterials. 2011 August ; 32(24): 5590–5599. doi:10.1016/j.biomaterials.2011.04.030.

Surface Functionalization of Hyaluronic Acid Hydrogels by Polyelectrolyte Multilayer Films

Seda Yamanlar[1,2,*], **Shilpa Sant**[1,2,3,*], **Thomas Boudou**[4], **Catherine Picart**[4], and **Ali Khademhosseini**[1,2,3,†]

[1] Center for Biomedical Engineering, Department of Medicine, Brigham and Women's Hospital, Harvard Medical School, 65 Landsdowne Street, Cambridge, MA 02139, USA

[2] Harvard-MIT Division of Health Sciences and Technology, Massachusetts Institute of Technology, Cambridge, MA 02139, USA

[3] Wyss Institute for Biologically Inspired Engineering, Harvard University, Boston, MA 02115 USA

[4] LMGP, Institut National Polytechnique de Grenoble et Centre National de la Recherche Scientifique, 3 parvis Louis Néel, F-38016 Grenoble, France

Abstract

Hyaluronic acid (HA), an anionic polysaccharide, is one of the major components of the natural extracellular matrix (ECM). Although HA has been widely used for tissue engineering applications, it does not support cell attachment and spreading and needs chemical modification to support cellular adhesion. Here, we present a simple approach to functionalize photocrosslinked HA hydrogels by deposition of poly(L-lysine) (PLL) and HA multilayer films made by the layer-by-layer (LbL) technique. PLL/HA multilayer film formation was assessed by using fluorescence microscopy, contact angle measurements, cationic dye loading and confocal microscopy. The effect of polyelectrolyte multilayer film formation on the physicochemical and mechanical properties of hydrogels revealed polyelectrolyte diffusion inside the hydrogel pores, increased hydrophobicity of the surface, reduced equilibrium swelling, and reduced compressive moduli of the modified hydrogels. Furthermore, NIH-3T3 fibroblasts seeded on the surface showed improved cell attachment and spreading on the multilayer functionalized hydrogels. Thus, modification of HA hydrogel surfaces with multilayer films affected their physicochemical properties and improved cell adhesion and spreading on these surfaces. This new hydrogel/PEM composite system may offer possibilities for various biomedical and tissue engineering applications, including growth factor delivery and co-culture systems.

†Correspondence should be addressed to: Ali Khademhosseini (alik@rics.bwh.harvard.edu), 65 Landsdowne Street, Cambridge, MA 02139, USA.
*Seda Yamanlar and Shilpa Sant contributed equally to this work.

Author Contribution

SS, CP and AK designed the study; SY and SS performed the experiments; TB performed the AFM nano-indentation experiments, SY and SS analyzed the data; SS and SY wrote the paper; SS, AK and CP revised the paper. All the authors discussed the results and commented on the paper.

Keywords

Hydrogels; Hyaluronic acid; Photocrosslinked; Surface functionalization; Layer-by-layer; Polyelectrolyte diffusion; Cell adhesion

1. Introduction

Hydrogels are attractive soft materials as three dimensional (3D) scaffolds for tissue engineering due to their structural and compositional similarities to natural extracellular matrix (ECM). Hydrogels typically imbibe 95–99% water and possess ECM-like viscoelastic and diffusive transport characteristics [1, 2]. The ability to engineer the properties of hydrogels such as cellular attachment, molecular response, structural integrity, biodegradability, biocompatibility and solute transport have enabled a wide range of new applications to interface with biological systems as a scaffold [1, 3–5]. Many hydrogel types with different physical and chemical properties have been developed using various synthetic approaches over the past several decades [1, 6].

HA is a linear anionic polysaccharide made of a repeated disaccharide of (1–3) and (1–4)-linked β-D-glucuronic acid and N-acetyl β-D-glucosamine monomer [7, 8]. It is the only non-sulphated glycosaminoglycan. HA plays important role in the organization and stabilization of ECM, cell proliferation (low M_w particularly) and differentiation [7, 9, 10]. HA is also involved in the morphogenesis, inflammation, and wound repair [11, 12]. Due to its importance *in vivo* and its potential in tissue engineering, several strategies have been developed to prepare HA-hydrogels including disulfide crosslinking [13] and photocrosslinking [14–16]. However, HA-based gels and HA-coated surfaces have been shown to be non-adhesive to cells and proteins *in vitro* [15, 17–19]. As the cell adhesion influences subsequent cell events such as proliferation and differentiation [20], it is important to fine tune the surface properties of hydrogels for tissue engineering applications.

In recent years, the deposition of polyelectrolyte multilayers (PEM) by layer-by-layer (LBL) technique has emerged as a promising tool for functionalization of various substrates owing to their ease of formation and flexibility of tailoring physicochemical properties [21]. PEM films involving HA as polyanion and a polypeptide, a polysaccharide or an ECM protein as polycation have been widely investigated, especially poly(L-lysine)/HA (PLL/HA) [22, 23], chitosan/HA (CHI/HA) [24]), and collagen/HA [25]. The pH-responsive properties of PLL/HA multilayer films have also been investigated [26, 27]. On the other hand, Khademhosseini and co-workers have patterned thin layers of HA in combination with PLL for generating stable *in vitro* co-cultures, by employing HA as a cell-repellent background and PLL as adhesive layer [19].

Given the versatility of PEMs, the development of PEM coatings on hydrogels is currently emerging as a useful tool to functionalize hydrogel surfaces for various biomedical applications. Sakaguchi et al. first reported the LBL deposition of PEMs on synthetic poly(vinyl alcohol) hydrogels to control their coagulant properties [28]. Recently, biomimetic stratified structures have been created by spray-deposition where PEMs were alternated with alginate gel layers containing cells to mimic multilayered 3D structures found in various tissues such as skin or cartilage [29]. On the other hand, Mehrotra et al have modified agarose hydrogels using synthetic polyelectrolytes built in a LbL manner to control the release of the model protein lysozyme from hydrogels [30]. While these examples demonstrate potential applications of LBL modified hydrogels as tailored surface coatings [28], biomimetic 3D architectures [29] and bioactive functionalized hydrogels for controlled drug release [30], there is no report to date on the effect of LbL deposition on the

microstructure, physicochemical and mechanical properties of a polysaccharide hydrogel. In this work, we investigated the surface functionalization of a cell- resistant HA hydrogel by sequential adsorption of PLL and HA to support the cell adhesion. The first objective of this work was to demonstrate the effective deposition of a PLL/HA film on the photocrosslinked HA hydrogel surface. The second objective was to investigate the physicochemical and mechanical properties of the PEM-coated hydrogel. Finally, we also evaluated the potential of such PEM-modified hydrogel surfaces to support fibroblast cell adhesion and spreading.

2. Materials and Methods

2.1. Synthesis of Methacrylated HA

Methacrylic anhydride (Aldrich, Milwaukee, WI) was reacted with a 100 mL of 10 % aqueous HA solution (molecular weight 7.4×10^5 g/mol; Lifecore Biomedical LLC, Chaska, MN) at 4 °C for 24 h while the pH was maintained in the range of 7.7–8.5 [31]. The synthesized methacrylated HA solution was dialyzed for 48 h at 4 °C, and lyophil ized for 72 h. The lyophilized product was stored at −20 °C until further use.

2.2. Preparation of HA Hydrogels

To build up multilayer films on the hydrogel surface, hydrogels were fabricated on glass slides treated with poly(3-trimethoxysilyl)propyl methacrylate (TMSPMA, Aldrich, Milwaukee, WI) [15]. Briefly, cleaned glass slides were coated with a 98% TMSPMA solution and incubated at 70°C for 12 h. The slides were then rinsed with distilled water to remove excess TMSPMA and dried. HA hydrogels were fabricated in poly(dimethyl siloxane) (PDMS, Sylgard 184, Essex Chemicals) molds (8 mm diameter, 2 mm height) placed on the methacrylated glass substrates. Hydrogels were prepared by exposing 70 μL of aqueous solution of methacrylated HA (5% w/v) containing 0.1% w/v photoinitiator (Irgacure: 2959, Ciba, Tarrytown, NY) to 6.9 mW/cm^2 UV light at 360–480 nm for 400 sec. Following UV exposure, PDMS molds were gently removed and hydrogels polymerized to the glass substrates were used to build polyelectrolyte layers on the exposed surface.

2.3. Polyelectrolyte Solutions

All polyelectrolytes were dissolved using NaCl solution (0.15 M) in ultrapure water (Mili-Q Ultra Pure Water System, Millipore). HA and PLL or PLL^{FITC} (Fluorescein isothiocyanate-poly(L-lysine), M_w=30,000–70,000 g/mol, Sigma, Milwaukee, WI) were dissolved at 1 mg/mL in 0.15 M NaCl solution. The pH of the polyelectrolyte solutions were maintained at 6.0–6.5. At this pH range, PLL is positively charged and HA is negatively charged [22]. The concentration of the polyelectrolyte solutions was kept constant at 1mg/mL and the concentration of NaCl solution was fixed at 0.15 M for all of the experiments during this study.

2.4. PLL/HA Multilayer Deposition

Multilayer formation on the hydrogel surface was performed manually. Hydrogels formed on TMSPMA glass slides were first allowed to swell at 37 °C in Dulbecco's phosphate buffered saline (DPBS) for 24 h. After swelling, they were gently rinsed with DPBS and introduced to the PLL^{FITC} solution for 7 min. Hydrogels were then rinsed in NaCl solution for 1 min and subsequently, introduced to HA solution for 7 min, followed by rinsing in NaCl solution for 1 min. After each step, the hydrogel was lightly blotted with a wipe to remove residual liquid. This procedure was repeated to build up 4 and 9 layer pairs of PLL/HA films ending with PLL, labeled henceforth as $(PLL/HA)_4$-PLL^{FITC} and $(PLL/HA)_9$-PLL^{FITC}, respectively. After the surface modification by LBL method, the gels were gently removed from the glass for further characterization.

2.5. Hydrogel Characterization

2.5.1. Analysis of Film Growth by Fluorescence Measurements—The $(PLL/HA)_i$ multilayer buildup process (*i* being the number of layer pairs) was evaluated by measuring the fluorescence intensity of PLL^{FITC}. The layers were built on the hydrogel surface with sequential deposition of PLL^{FITC} and HA by dip-coating (Fig. 1). After the deposition of each layer, hydrogel surface was imaged with an inverted fluorescence microscope (Nikon TE 2000-U, Nikon Instruments Inc., USA) and the fluorescence intensity of each image was calculated by using ImageJ software (NIH, http://rsbweb.nih.gov/ij/index.html). Three images were taken for five hydrogel samples after each layer buildup.

2.5.2. Contact Angle Measurement—After deposition of each PLL and HA layer, static water contact angles were measured with a DSA100 contact angle measurement system (Kruss, Hamburg, Germany) using 10 μl deionized water droplet. The air-water contact angles were determined by using ImageJ software.

2.5.3. Methylene Blue (MB) Adsorption—The hydrogels without and with multilayers were stained with a cationic dye, methylene blue (MB), to confirm layer formation. Unmodified hydrogels, $(HA)_0$ and hydrogels coated with films were immersed in MB solution (0.002 wt %) for 10 min, $(PLL/HA)_4$-PLL, $(PLL/HA)_9$-PLL followed by immersion in DPBS for 3 days to allow diffusion of dye [28].

2.5.4. Confocal Laser Scanning Microscopy (CLSM)—The thickness of (PLL^{FITC}/HA) multilayer films was measured by Confocal Laser Scanning Microscopy (CLSM) (Olympus FV300, Meville, NY) using 20X objective and 0.5 μm *z*-intervals. FITC fluorescence was detected upon excitation at 488 nm, through a cut-off dichroic mirror and an emission band-pass filter of 505–530 nm.

2.5.5. Scanning Electron Microscopy (SEM)—The microstructure of HA hydrogels with/without multilayer films was observed using Scanning Electron Microscope (SEM) EVO 55 (Carl Zeiss, Inc. NY). Hydrogels were flash-frozen using liquid nitrogen and lyophilized [32]. Dried hydrogels were sputter-coated with ion coater (Cressington, Cranberry Twp., PA) using palladium-platinum target materials. For ion coating, ion current was controlled to 40 mA for 90 sec for $(HA)_0$ samples and 40 mA for 270 sec for multilayered samples (n=3) prior to morphological examination under ESEM. The images were captured at 25kV. For $(HA)_0$ and $(PLL/HA)_4$-PLL samples, the images were taken under high vacuum mode using secondary electron (SE) detector. However, for $(PLL/HA)_9$-PLL, it was difficult to take images under high pressure mode using SE detector due to higher electrical charges. Thus, the images were taken under variable pressure mode using backscattered electron (BS) detector that is less affected by electric charge.

2.5.6 Swelling Measurement—For the swelling studies, hydrogel samples were immersed in DPBS at 37 °C for predetermined time, removed from DPBS, gel surfaces were quickly wiped to remove the residual liquid and swollen weight was recorded for different time points (n=4) up to 48 h. After 48h, samples were dried in a vacuum oven at 80 °C for 3 days and weig hed once more to determine the dry weight of HA. The swelling ratio was then calculated as the ratio of swollen hydrogel mass to the dry weight of HA.

2.5.7. Mechanical Testing—To evaluate the effect of multilayer formation on the mechanical properties of the hydrogels, unconfined compression tests were performed on Instron 5542 mechanical tester (Norwood, MA). 200 μL of polymer solution mixed with photoinitiator were placed between two glass slides separated by a 2 mm spacer and exposed to 6.9 mW/cm^2 UV light (360–480 nm) for 400 sec. Hydrogel samples were removed from

glass slides gently and allowed to swell in DPBS at 37 °C for 24 h. A biopsy punch was used to generate 8 mm discs to form three sets from swollen hydrogel sheet (n=5). Then, two sets were used to build up $(PLL/HA)_i$ multilayers on the hydrogel surface. Before testing, the hydrogel sample was wiped lightly and compressed at a rate of 0.2 mm per minute until failure. The Young's modulus was defined as the slope of the initial linear region of the stress-strain curve in the first 5–15% strain range.

2.6. Cell Culture

NIH-3T3 cells were cultured in Dulbecco's modified Eagle medium (DMEM, Invitrogen, Carlsbad, CA) supplemented with 10% fetal bovine serum and 1% penicillin–streptomycin (Invitrogen) in a 5% CO_2, 37 °C incubator. For surface adhesion studies, hy drogel samples were placed in PDMS molds and covered with 200 μL of cell suspension containing 500,000 cells/mL for 3h, washed with DPBS and cultured normally (n=5). A calcein-AM/ethidium homodimer Live/Dead assay (Invitrogen) was used to assess the cell viability according to the manufacturer's instructions. After 48 h, samples were incubated with DPBS containing 2 μM calcein and 4 μM ethidium homodimer for 15 min (37 °C, 5% CO_2), washed with DPBS three times, and imaged with an inverted fluorescence microscope (Nikon TE 2000-U, Nikon instruments inc., USA). For assessment of cell spreading, cells were fixed with 4% paraformaldehyde and stained with phalloidin (Alexa-Fluor 594, Invitrogen) and DAPI to visualize F-actin filaments and cell nuclei, respectively. Total cell number was quantified using ImageJ (NIH, http://rsbweb.nih.gov/ij/index.html) by counting DAPI stained nuclei. The shape index of each individual cell nucleus representing nuclear elongation was analyzed using ImageJ software, with a shape index of 1 representing a circle [33].

Data Analysis

Statistical significance was determined by Student's t-test for two groups of data or analysis of variance (ANOVA) followed by Fisher's LSD post hoc test for multiple comparisons using PASW Statistics 18 (SPSS Inc., IBM Chicago, Illinois). For all statistical tests, the level of significance was set at $p<0.05$. Data are presented as mean $^{+}$ standard deviation (SD).

3. Results and Discussion

3.1. PLL/HA Multilayer Growth on HA Hydrogel

Figure 1 represents the schematics of multilayer buildup process on HA hydrogel with the alternate deposition of PLL and HA by manual dip-coating. As many properties of PEM films formed from weak polyelectrolytes (i.e. alginate, chitosan, poly(L-lysine), poly(glutamic acid), hyaluronan, etc.) are strongly dependent on the pH and ionic strength of the polyelectrolyte solutions, these parameters were fixed at 0.15 M NaCl at pH 6.0–6.5 to build up stable PLL/HA multilayer films on hydrogel surface. In such conditions, film growth on a planar glass substrate has previously been characterized by atomic force microscopy, zeta potential and quartz crystal microbalance [21]. It is important for LBL technique to provide the main driving forces for assembly of the films, not only for the multilayer formation on the surface but also to effectively anchor the multilayers to the underlying substrate. HA has one carboxylic acid group per disaccharide unit whereas PLL has one amino group per monomer repeat unit [23] and the electrostatic interaction between these groups as well as secondary interactions, such as hydrogen bonds, makes it possible to form PLL/HA multilayers on the hydrogel. Therefore, during the first deposition step, interaction between negatively charged free carboxylic acid groups in HA hydrogel with positively charged amino groups in PLL was used to adsorb a layer of PLL on the hydrogel surface to generate an anchorage layer [34].

PLL/HA multilayer growth on the outermost surface of HA hydrogel was assessed by the changes in fluorescent intensity, contact angle and the adsorption of the cationic MB dye during the build up process. To this end, we employed fluorescently labeled PLL (PLL^{FITC}) as the polycationic layer to enable easy visualization of the multilayer growth [22]. The fluorescent images taken following each (PLL^{FITC}/HA) deposition step were analyzed for the fluorescent intensity using ImageJ (Fig. 2A). The statistically increased fluorescent intensity during the construction of $(PLL/HA)_i$-PLL^{FITC} (i=1, 4 and 9) indicated multilayer growth of PLL/HA on the hydrogel surface with the increased number of assembly steps (Fig. 2B, One-way ANOVA, $p<0.05$).

We further studied the multilayer growth by contact angle measurements with each PLL and HA deposition step (Fig. 2C). The static water contact angle of the uncoated HA hydrogel was determined to be 36.5 ± 2°, which changed to 44 ± 2 ° after first layer of PLL deposition. Subsequent deposition of each HA and PLL layers exhibited similar trends showing low and high contact angles for HA and PLL, respectively. Thus, the polycationic PLL layers were more hydrophobic than the polyanionic HA ones. Our results are supported by previous studies where PLL showed higher contact angle values than HA when HA/PLL layers were built on chitosan substrate [35]. Similarly, Kolasinska et al have observed that polycation (PLL) terminated multilayers were more hydrophobic than polyanion (PGA) terminated ones [36]. The authors suggested that the electric charge density is lower when polycation forms the outermost layer. The other possible reason suggested was more favorable orientation of water molecules at the negatively charged surfaces [36]. With subsequent deposition of PLL and HA, contact angle oscillated between low and high values indicating the multilayer buildup on the outer surface of the hydrogel. For first three layer pairs, there was no significant change in contact angle values from HA_1 to HA_3 and PLL_1 to PLL_3 (One-way ANOVA, Fisher's LSD, $p>0.05$). However, when the number of the layer pairs increased further, the contact angle in each deposition step also increased significantly (One-way ANOVA, Fisher's LSD, $p < 0.05$) compared to previous corresponding layer (HA_3 *Vs* HA_4; PLL_3 *Vs* PLL_4 and PLL_5). It was noted that layer-to-layer variations of the contact angle were regular for first two layer pairs, $(PLL/HA)_2$ and became irregular thereafter. The observed irregular oscillations can be due to the interlayer mixing during PLL/HA film growth. It has been previously reported that PLL/HA films grow exponentially due to diffusion of mobile PLL chains in and out of the layers [22, 37]. Kolasinska et al have observed similar irregular oscillations in contact angles for another exponentially growing film, PLL/PGA, which was attributed to higher mixing between polymer layers [36].

To further observe the multilayer formation on the hydrogel surface, the unmodified and modified hydrogels were stained with a cationic MB after immersion in the dye solution for 10 min followed by 3 days of immersion in DPBS as described previously [28] (Fig. 2D). The unmodified hydrogel, $(HA)_0$, exhibited light blue color showing some adsorption of dye inside the bulk of the hydrogels due to its interaction with the charged carboxylate groups of HA molecules. However, blue color intensity of the PEM-coated hydrogel increased with increased number of layer pairs (i=4, 9). It has previously been established that the permeable film structure and binding sites are necessary for MB to be loaded into the films [38, 39]. Thus, the amount of MB adsorption is determined by the availability of free carboxylate groups within the surface layer, i.e., those not bound to ammonium groups of polycations. Increased MB adsorption (Fig. 2D) suggested that number of available free carboxylate groups increased with the number of layer pairs. This is expected because the amount of HA molecules increases with deposition of each HA layer and possibly, all the carboxylate groups of deposited HA molecules are not ionically crosslinked with ammonium groups of neighboring PLL molecules. Thus, HA may be engaged in loose interactions with PLL and some HA carboxylate groups may be unpaired leading to MB adsorption inside the multilayer structure [38]. Another reason for more MB adsorption and retention inside the

modified hydrogels may be the altered permeability of the hydrogel and multilayer structure. This will be discussed in more details in section 3.3.

3.2. Effect of Solution Dipping Time and Number of Layer Pairs on the PEM Film

Thickness To estimate the PEM film thickness, we imaged a film that contained PLL^{FITC} as a tracer by using CLSM. We first investigated the effect of dipping time on $(PLL/HA)_4$-PLL^{FITC} multilayer films (Fig. 3A). As the adsorption time of the polyelectrolytes increased, the thickness of the green band corresponding to PLL-FITC increased notably. We also noted that, while keeping the adsorption time constant (7 min), the film thickness increased significantly with the number of layers, from 19.8 μm for a $(PLL/HA)_4$-PLL^{FITC} to 35.8 μm for a $(PLL/HA)_9$-PLL^{FITC} film (Fig. 3B). It is expected that increasing the number of layers increases the exposure time. But, as the layers build, they will also act as barrier to prevent further diffusion inside the bulk of the gel. Confocal sections demonstrated a homogeneous fluorescence of PLL^{FITC} throughout the entire film thickness. This may be attributed to the diffusion of mobile PLL^{FITC} chains in and out of the film due to interlayer mixing of HA and PLL^{FITC} [22]. In fact, it has previously been shown that polyelectrolyte systems composed of synthetic polyelectrolytes such as poly(allylamine)/poly(styrenesulfonate) or poly(diallyldimethylammonium)/poly(styrenesulfonate) grow linearly with the number of deposited layers, while others composed of natural polyelectrolytes like polyaminoacids (poly(glutamic acid), PLL, poly(aspartic acid)) or polysaccharides (alginate, HA, chitosan, chondroitin sulfate) reveal an “exponential growth regime” [21]. In the case of PLL/HA films, inward and outward diffusion of PLL^{FITC} throughout the film [22, 37] led to the visualization of a homogeneous fluorescence throughout the entire film thickness. This further supports the contact angle data where irregular oscillations in contact angle were attributed to the interlayer mixing of two polyelectrolytes as discussed in the previous section.

3.3. Effect of PEM Growth on the Physicochemical and Mechanical Properties of HA Hydrogels

We also investigated the effect of the PEM film growth on the physicochemical and mechanical properties of the modified hydrogels. Lyophilized hydrogel sections prepared for the unmodified hydrogel $(HA)_0$, and for the film-coated hydrogels (respectively $(PLL/HA)_4$-PLL and $(PLL/HA)_9$-PLL assemblies) were visualized by SEM. Figure 4 illustrates the differences in the surface and bulk structure of the hydrogels before and after multilayer construction. The top surface of $(HA)_0$ hydrogels showed smooth flakey structure (Fig. 4, left column) whereas modified hydrogel surfaces showed a more rough granular structure (Fig. 4, middle and right columns). Similarly, the cross-section revealed relatively homogeneous and uniform structure throughout the section of $(HA)_0$ gels (Fig. 4, middle row). The outer surface of modified hydrogels showed formation of the film (labeled as L in Fig. 4), with increased film thickness for $(PLL/HA)_9$-PLL as compared to $(PLL/HA)_4$-PLL. Thus SEM images supported the previous results obtained by CLSM (Fig. 3). The bulk structure of the gel cross-sections (Fig. 4, bottom row) confirmed the diffusion of the polyelectrolytes inside of the hydrogels (indicated by white arrows). When the HA hydrogel was first brought into contact with the PLL solution (Fig. 1), polycations (PLL) diffused partially into the bulk hydrogel structure, possibly forming the initial phase of multilayer growth inside the intrinsic pores due to negatively charged HA [30]. However, as the deposition steps increased, the layers were formed on the surface masking the hydrogel pores as confirmed by the SEM images (Fig. 4, top row). In summary, the sequential deposition of PLL/HA layer pairs resulted in the formation of a film on the outermost surface of the HA hydrogel, with an initial phase of polyelectrolyte diffusion inside the bulk hydrogels.

Polyelectrolyte diffusion inside of the pores can affect swelling and mechanical properties of the resultant PEM-coated hydrogels. Hence, the swelling tests were performed in DPBS for each group of samples, $(HA)_0$, $(PLL/HA)_4$-PLL and $(PLL/HA)_9$-PLL. We observed that PEM-coated hydrogels displayed a significantly lower degree of swelling ($p<0.05$) as compared to the $(HA)_0$ hydrogels, while there was no significant effect of the number of layers on the swelling ratio (Fig. 5A and B). This could be explained on the basis of polyelectrolyte diffusion inside the pores as well as increased hydrophobicity of the surfaces. As discussed previously, the microstructure of hydrogels (Fig. 4, middle row) showed interpenetration of polyelectrolytes inside the pores during multilayer formation, causing their partial or complete blockage, potentially affecting the swelling properties of the PEM-coated hydrogels. In addition, contact angle measurements suggested that PLL increased the surface hydrophobicity (Fig. 1C). Thus, overall surface hydrophobicity and pore structure might contribute to the reduced equilibrium swelling for the modified hydrogels. Indeed, it has been suggested that swelling/shrinking of polyelectrolyte PEM capsules is determined by two compelling forces, namely, electrostatic and hydrophobic forces [40]. When hydrophobic forces dominate, the tendency to reduce the polymer/water interface leads to the reduced swelling. The reduced permeability of PEM-coated hydrogels may be another possible reason for increased MB retention inside these hydrogels (Fig. 2D).

We further investigated the mechanical properties of the hydrogels as a function of the thickness of PEM coatings. In all three conditions, the hydrogels exhibited similar stress-strain behavior, irrespective of number of layer pairs (Fig. 6A). However, multilayer growth on the hydrogel surface led to a significant decrease in the Young's modulus calculated from 5–15% strain region ($p <0.05$, Fig. 6B). A significant increase in compressive stress and strain properties at break was also noticed ($p <0.05$, Fig. 6C and D). While both the $(PLL/HA)_4$-PLL and $(PLL/HA)_9$-PLL hydrogels showed significantly greater failure properties as compared to $(HA)_0$ hydrogels, there were no significant differences between PEM-coated hydrogels (n=4 or 9). As PEM film formation caused a decrease in swelling and water transport, the ultimate properties could be affected by the decreased water mobility in multilayered structure. Also, the presence of the multilayers on the surface could directly improve the stress handling capabilitiesof the modified hydrogels by providing a reinforcing layer on the outer surface. At lower compressive strains (5–15%), presence of PLL may lead to some charge shielding, decreasing the chain repulsions and resulting in elastic behavior (Fig. 6B). On the other hand, increased compressive strengths observed at higher strains (Fig. 6C) may be attributed to the increased polymer network density due to hydrogel shrinking (Fig. 5). However, in all conditions, the general stress-strain behavior was similar; suggesting that while there were significant changes in the compressive modulus and ultimate stress/strain, overall mechanical behavior was similar for modified and unmodified hydrogels (Fig. 6A). This suggests that the observed changes in the mechanical properties may be due to the modification of only the surfaces of the hydrogels with less effect on the bulk hydrogel properties. This was indeed confirmed by AFM nano-indentation experiments, which evidenced the presence of a bi-regime indentation curve and could not be fitted by a single value for the Young's modulus (data not shown).

3.4. Cell Viability and Adhesion on Modified HA Hydrogel Surface

A major challenge in tissue engineering is to obtain the controlled or desired cell adhesion under physiological conditions through optimized surface characteristics as cell adhesion influences subsequent cell events such as proliferation and differentiation [20]. Although HA is an important component of ECM, HA hydrogels are known to poorly support cell adhesion and usually need additional chemical modification with RGD sequences [41, 42]. We studied the ability of HA hydrogels with or without PEM coatings to support the cell viability and cell adhesion, without using any additional peptide sequence. NIH 3T3

fibroblasts were seeded on the surface of hydrogels and allowed to attach for 3 h, washed with DPBS to remove unattached cells and cultured for additional time. After 48 h, cell viability studies were carried out on the cells seeded on the hydrogels with $(HA)_0$ and $(PLL/HA)_4$-PLL and $(PLL/HA)_9$-PLL films using live/dead assay kit. As shown in Fig. 7A, the cells remained viable (green) with few dead (red) cells indicating good cytocompatibility of the films formed on the hydrogels. Unmodified hydrogels $(HA)_0$ exhibited significantly lower cell attachment, with most cells remaining detached from the surface as expected for HA hydrogels without surface treatment (Fig. 7B and C). Image analysis using DAPI and phalloidin staining showed significantly higher number of cells attached on the modified hydrogels as compared to the unmodified ones (ANOVA $p<0.05$). We observed a significant increase in cell adhesion when the number of layer pairs was increased from 4 to 9 (Fig. 7B, C, and D, ANOVA $p<0.05$). Furthermore, the cells were also more spread with elongated nuclei, as indicated by a lower nuclear shape index.

In their previous studies, Richert and co-authors found that cells neither adhered nor spread on the un-crosslinked native PLL/HA films deposited on glass substrates irrespective of the nature of the topmost layer [43, 44]. On the other hand, carbodiimide (EDC)-crosslinked films favorably supported cell adhesion and proliferation. This difference was attributed to the rigidity of the crosslinked films. Given that the unmodified hydrogel and PLL/HA films alone do not support cell adhesion and spreading, our results indicated that PLL/HA films built on HA hydrogels showed favorable cell response (Fig. 7). We hypothesize that this is due to the intermixing of the polyelectrolytes and the hydrogels, which altered the physicochemical properties of the hydrogel surface to render it cell adhesive. Indeed, surface hydrophilicity, hydration and swellability as well as surface roughness are considered to be important for cell attachment and protein adsorption [43]. As discussed previously, PEM-film deposition decreased the swelling of the hydrogels and considerably modified their outermost surface. From SEM images (Fig. 4), an increased surface roughness is observed after LbL deposition on the HA hydrogel. In addition, the contact angle increased with multilayer number indicating increased surface hydrophobicity, which correlated well with increased cell attachment. All together, our data suggest that the presence of PLL/HA multilayers promote cell adhesion and spreading on the hydrogel surface, making HA hydrogels more suitable for tissue engineering studies.

The developed composite hydrogel/PEM film system offers possibilities for various biomedical and tissue engineering applications. For instance, PEM films on the hydrogel surface may offer controlled protein/growth factor release to the cells encapsulated in the hydrogels as LbL films are known to trap or retain active forms of various types of growth factors (including basic fibroblast growth factors [45, 46], vascular endothelial growth factor [47], or bone morphogenetic protein 2 [48]). Another possibility would be to develop a co-culture system that mimics biological systems. This could be employed to study epithelial-mesenchymal interactions that occur during development and morphogenesis or endothelial cells/osteoblast interactions that occur during bone regeneration.

4. Conclusion

We constructed PEM films on the surface of photocrosslinked HA hydrogels and investigated the effect of multilayer growth on the physicochemical and mechanical properties of the HA hydrogels. Fluorescence microscopy and contact angle measurements confirmed that the HA hydrogel surface was modified after deposition of each PLL and HA layers. We observed that the PEM film thickness increased with the adsorption time as well as with the number of deposited layer pairs. Scanning electron microscopy images revealed the presence of film infiltrating and covering the porous hydrogel surface. The equilibrium swelling decreased while failure stress/strain increased after surface modification of

hydrogels with polyelectrolytes. Consequently, modified physicochemical properties supported the cell attachment and spreading on the hydrogel surface, highlighting its potential applications in tissue engineering.

Acknowledgments

This research was funded by the National Institutes of Health (EB009196; DE019024; EB007249; HL099073; AR057837), the National Science Foundation CAREER Award (DMR0847287) and the Office of Naval Research Young Investigator Award. SS was supported partly by a postdoctoral fellowship from Fonds de Recherche sur la Nature et les Technologies (FQRNT), Quebec, Canada. C.P. is indebted to the Institut Universitaire de France for financial support. We extend our sincere thanks to Dr. Che B. Hutson, Dr. Jason W. Nichol, and Brenna Nichol for their excellent comments and feedback on the manuscript. We also thank Halil Tekin for help with contact angle measurements and Dr. Thomas Crouzier for initial fruitful discussions.

References

1. Slaughter BV, Khurshid SS, Fisher OZ, Khademhosseini A, Peppas NA. Hydrogels in regenerative medicine. Adv Mater. 2009; 21(32–33):3307–3329. [PubMed: 20882499]
2. Peppas NA, Hilt JZ, Khademhosseini A, Langer R. Hydrogels in biology and medicine: From molecular principles to bionanotechnology. Adv Mater. 2006; 18(11):1345–1360.
3. Mooney, DJ.; Langer, RS. Engineering biomaterials for tissue engineering: The 10–100 micron size scale. In: Bronzino, DJ., editor. The biomedical engineering handbook. Boca Raton: CRC Press LLC; 2000.
4. Khademhosseini A, Langer R. Microengineered hydrogels for tissue engineering. Biomaterials. 2007; 28:5087–5092. [PubMed: 17707502]
5. Sant S, Hancock MJ, Donnelly JP, Iyer D, Khademhosseini A. Biomimetic gradient hydrogels for tissue engineering. Can J Chem Eng. 2010; 88(6):899–911.
6. Miller, JS.; West, JL. Micro and nanoengineering of the cell microenvironment. Artech House; 2008. Biomimetic hydrogels to support and guide tissue formation; p. 101-120.
7. Rabanel, JM.; Bertrand, N.; Sant, S.; Louati, S.; Hildgen, P. Polysaccharide hydrogels for the preparation of immunoisolated cell delivery systems. In: Marchessault, RH.; Ravenelle, F.; Zhu, XX., editors. Polysaccharides for drug delivery and pharmaceutical applications. Washington: American Chemical Society; 2006. p. 305-339.
8. Masters KS, Shah DN, Leinwand LA, Anseth KS. Crosslinked hyaluronan scaffolds as a biologically active carrier for valvular interstitial cells. Biomaterials. 2005; 26(15):2517–2525. [PubMed: 15585254]
9. Fraser JRE, Laurent TC, Laurent UBG. Hyaluronan: Its nature, distribution, functions and turnover. J Intern Med. 1997; 242(1):27–33. [PubMed: 9260563]
10. Burdick JA, Chung C, Jia XQ, Randolph MA, Langer R. Controlled degradation and mechanical behavior of photopolymerized hyaluronic acid networks. Biomacromolecules. 2005; 6(1):386–391. [PubMed: 15638543]
11. Tool BP. Hyaluronan in morphogenesis. Semin Cell Develop Biol. 2001; 12(2):79–87.
12. Chen WYJ, Abatangelo G. Functions of hyaluronan in wound repair. Wound Repair Regen. 1999; 7(2):79–89. [PubMed: 10231509]
13. Shu XZ, Ahmad S, Liu YC, Prestwich GD. Synthesis and evaluation of injectable, in situ crosslinkable synthetic extracellular matrices for tissue engineering. J Biomed Mater Res A. 2006; 79A(4):902–912. [PubMed: 16941590]
14. Nettles DL, Vail TP, Morgan MT, Grinstaff MW, Setton LA. Photocrosslinkable hyaluronan as a scaffold for articular cartilage repair. Ann Biomed Eng. 2004; 32(3):391–397. [PubMed: 15095813]
15. Khademhosseini A, Eng G, Yeh J, Fukuda J, Blumling J, Langer R, et al. Micromolding of photocrosslinkable hyaluronic acid for cell encapsulation and entrapment. J Biomed Mater Res A. 2006; 79A(3):522–532. [PubMed: 16788972]

16. Seidlits SK, Khaing ZZ, Petersen RR, Nickels JD, Vanscoy JE, Shear JB, et al. The effects of hyaluronic acid hydrogels with tunable mechanical properties on neural progenitor cell differentiation. Biomaterials. 2010; 31(14):3930–3940. [PubMed: 20171731]

17. Pavesio A, Renier D, Cassinelli C, Morra M. Anti-adhesive surfaces through hyaluronan coatings. Med Device Technol. 1997; 8(7):20–21. 24–27. [PubMed: 10174199]

18. Morra M, Cassineli C. Non-fouling properties of polysaccharide-coated surfaces. J Biomat Sci-Polym E. 1999; 10(10):1107–1124.

19. Khademhosseini A, Suh KY, Yang JM, Eng G, Yeh J, Levenberg S, et al. Layer-by-layer deposition of hyaluronic acid and poly-l-lysine for patterned cell co-cultures. Biomaterials. 2004; 25(17):3583–3592. [PubMed: 15020132]

20. Burridge K, Chrzanowska Wodnicka M. Focal adhesions, contractility, and signaling. Ann Rev Cell Develop Biol. 1996; 12:463–518.

21. Boudou T, Crouzier T, Ren KF, Blin G, Picart C. Multiple functionalities of polyelectrolyte multilayer films: New biomedical applications. Adv Mater. 2010; 22(4):441–467. [PubMed: 20217734]

22. Picart C, Mutterer J, Richert L, Luo Y, Prestwich GD, Schaaf P, et al. Molecular basis for the explanation of the exponential growth of polyelectrolyte multilayers. P Natl Acad Sci USA. 2002; 99(20):12531–12535.

23. Picart C, Lavalle P, Hubert P, Cuisinier FJG, Decher G, Schaaf P, et al. Buildup mechanism for poly(l-lysine)/hyaluronic acid films onto a solid surface. Langmuir. 2001; 17(23):7414–7424.

24. Thierry B, Kujawa P, Tkaczyk C, Winnik FM, Bilodeau L, Tabrizian M. Delivery platform for hydrophobic drugs: Prodrug approach combined with self-assembled multilayers. J Am Chem Soc. 2005; 127(6):1626–1627. [PubMed: 15700982]

25. Zhang J, Senger B, Vautier D, Picarta C, Schaaf P, Voegel J-C, Lavalle P. Natural polyelectrolyte films based on layer-by layer deposition of collagen and hyaluronic acid. Biomaterials. 2005; 26:3353–3361. [PubMed: 15603831]

26. Burke SE, Barrett CJ. Ph-responsive properties of multilayered poly(l-lysine)/hyaluronic acid surfaces. Biomacromolecules. 2003; 4(6):1773–1783. [PubMed: 14606908]

27. Morra M. Engineering of biomaterials surfaces by hyaluronan. Biomacromolecules. 2005; 6(3): 1205–1223. [PubMed: 15877335]

28. Sakaguchi H, Serizawa T, Akashi M. Layer-by-layer assembly on hydrogel surfaces and control of human whole blood coagulation. Chem Lett. 2003; 32(2):174–175.

29. Grossin L, Cortial D, Saulnier B, Felix O, Chassepot A, Decher G, et al. Step-by-step build-up of biologically active cell-containing stratified films aimed at tissue engineering. Adv Mater. 2009; 21(6):650–655.

30. Mehrotra S, Lynam D, Maloney R, Pawelec KM, Tuszynski MH, Lee I, et al. Time controlled protein release from layer-by-layer assembled multilayer functionalized agarose hydrogels. Adv Funct Mater. 2010; 20(2):247–258. [PubMed: 20200599]

31. Brigham MD, Bick A, Lo E, Bendali A, Burdick JA, Khademhosseini A. Mechanically robust and bioadhesive collagen and photocrosslinkable hyaluronic acid semi-interpenetrating networks. Tissue Eng PT A. 2009; 15(7):1645–1653.

32. Hwang CM, Sant S, Masaeli M, Kachouie NN, Zamanian B, Lee SH, et al. Fabrication of three-dimensional porous cell-laden hydrogel for tissue engineering. Biofabrication. 2010; 2(3)

33. Aubin H, Nichol JW, Hutson CB, Bae H, Sieminski AL, Cropek DM, et al. Directed 3d cell alignment and elongation in microengineered hydrogels. Biomaterials. 2010; 31(27):6941–6951. [PubMed: 20638973]

34. Mjahed H, Porcel C, Senger B, Chassepot A, Netter P, Gillet P, et al. Micro-stratified architectures based on successive stacking of alginate gel layers and poly(l-lysine)-hyaluronic acid multilayer films aimed at tissue engineering. Soft Matter. 2008; 4(7):1422–1429.

35. Hahn SK, Hoffman AS. Preparation and characterization of biocompatible polyelectrolyte complex multilayer of hyaluronic acid and poly-l-lysine. Int J Biol Macromol. 2005; 37(5):227–231. [PubMed: 16405994]

36. Kolasinska M, Warszynski P. The effect of nature of polyions and treatment after deposition on wetting characteristics of polyelectrolyte multilayers. Appl Surf Sci. 2005; 252(3):759–765.

37. Lavalle P, Vivet V, Jessel N, Decher G, Voegel JC, Mesini PJ, et al. Direct evidence for vertical diffusion and exchange processes of polyanions and polycations in polyelectrolyte multilayer films. Macromolecules. 2004; 37(3):1159–1162.
38. Chung AJ, Rubner MF. Methods of loading and releasing low molecular weight cationic molecules in weak polyelectrolyte multilayer films. Langmuir. 2002; 18(4):1176–1183.
39. Yoo D, Shiratori SS, Rubner MF. Controlling bilayer composition and surface wettability of sequentially adsorbed multilayers of weak polyelectrolytes. Macromolecules. 1998; 31(13):4309–4318.
40. Kohler K, Mohwald H, Sukhorukov GB. Thermal behavior of polyelectrolyte multilayer microcapsules: 2. Insight into molecular mechanisms for the pdadmac/pss system. J Phys Chem B. 2006; 110(47):24002–24010. [PubMed: 17125370]
41. Masters KS, Shah DN, Walker G, Leinwand LA, Anseth KS. Designing scaffolds for valvular interstitial cells: Cell adhesion and function on naturally derived materials. J Biomed Mater Res A. 2004; 71A(1):172–180. [PubMed: 15368267]
42. Shu XZ, Ghosh K, Liu YC, Palumbo FS, Luo Y, Clark RA, et al. Attachment and spreading of fibroblasts on an rgd peptide-modified injectable hyaluronan hydrogel. J Biomed Mater Res A. 2004; 68A(2):365–375. [PubMed: 14704979]
43. Richert L, Boulmedais F, Lavalle P, Mutterer J, Ferreux E, Decher G, et al. Improvement of stability and cell adhesion properties of polyelectrolyte multilayer films by chemical cross-linking. Biomacromolecules. 2004; 5(2):284–294. [PubMed: 15002986]
44. Richert L, Schneider A, Vautier D, Vodouhe C, Jessel N, Payan E, et al. Imaging cell interactions with native and crosslinked polyelectrolyte multilayers. Cell Biochem Biophys. 2006; 44(2):273–285. [PubMed: 16456228]
45. Macdonald ML, Rodriguez NM, Shah NJ, Hammond PT. Characterization of tunable fgf-2 releasing polyelectrolyte multilayers. Biomacromolecules. 2010; 11(8):2053–2059. [PubMed: 20690713]
46. Almodovar J, Bacon S, Gogolski J, Kisiday JD, Kipper MJ. Polysaccharide-based polyelectrolyte multi layer surface coatings can enhance mesenchymal stem cell response to adsorbed growth factors. Biomacromolecules. 2010; 11(10):2629–2639. [PubMed: 20795698]
47. Muller S, Koenig G, Charpiot A, Debry C, Voegel JC, Lavalle P, et al. Vegf-functionalized polyelectrolyte multilayers as proangiogenic prosthetic coatings. Adv Funct Mater. 2008; 18(12):1767–1775.
48. Crouzier T, Ren K, Nicolas C, Roy C, Picart C. Layer-by-layer films as a biomimetic reservoir for rhbmp-2 delivery: Controlled differentiation of myoblasts to osteoblasts. Small. 2009; 5(5):598–608. [PubMed: 19219837]

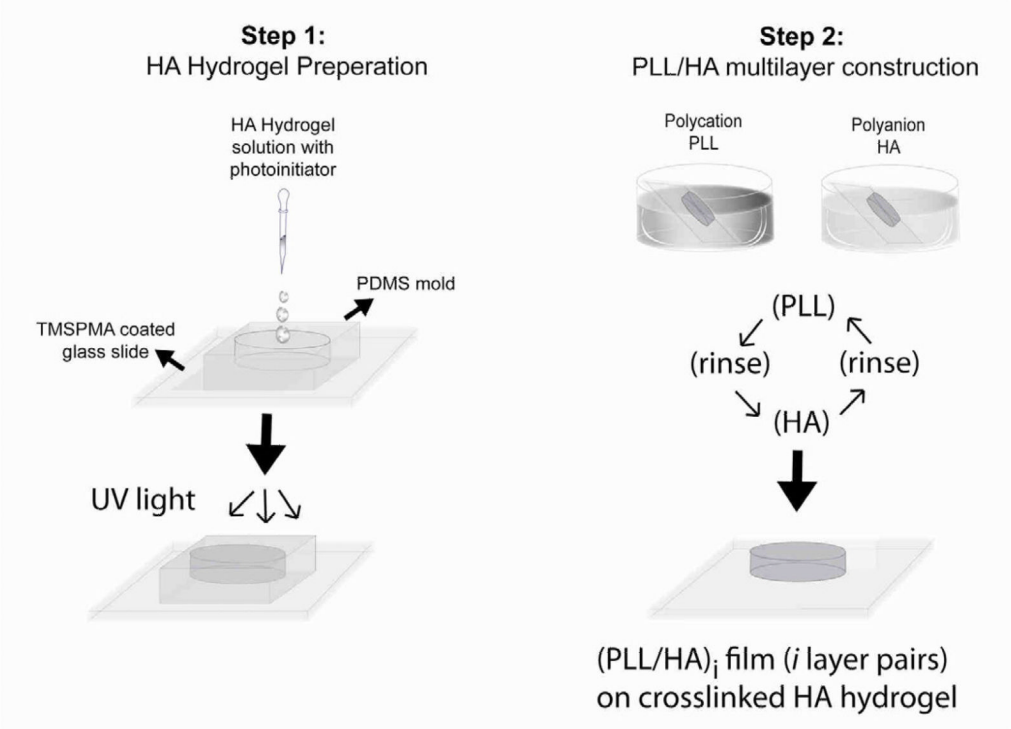

Figure 1.

Schematic of the photocrosslinked HA hydrogel formation and LBL assembly process on the hydrogel surface. In step 1, the methacrylated HA hydrogel is formed on a TMSPMA-coated glass slide using a PDMS mold and UV irradiation. In step 2, the PLL/HA multilayer film is formed by dipping the crosslinked hydrogel alternatively in PLL and HA solutions. The hydrogel surface is rinsed after each deposition of a polycation or polyanion layer.

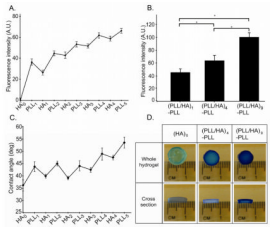

Figure 2.

Evaluation of the LBL assembly process on HA hydrogel surfaces. **A.** Fluorescence intensity of PLL^{FITC} after each step of the multilayer formation. The deposited layers led to an increase of PLL^{FITC} fluorescence. **B.** Bar graph showing fluorescence intensity of PLL^{FITC} layers after assembly of $(PLL/HA)_1$-PLL^{FITC}, $(PLL/HA)_4$-PLL^{FITC}, $(PLL/HA)_9$-PLL^{FITC} on the hydrogel surface (One-Way ANOVA, post-hoc analysis by Fisher' LSD, * $p<0.01$). Fluorescence intensity increased with the number of layer pairs. **C.** Contact angle measurements after each layer deposition step on HA hydrogels. Deposition of HA reduced the contact angle whereas PLL layer increased the contact angle of HA hydrogel surface in an alternating manner. **D.** Photographs showing different degrees of the adsorption of cationic dye, methylene blue (MB) in the PEM-coated hydrogel. $(PLL/HA)_4$-PLL and $(PLL/HA)_9$-PLL films showed increased adsorption of MB, which was stable even after immersion in water for 3d.

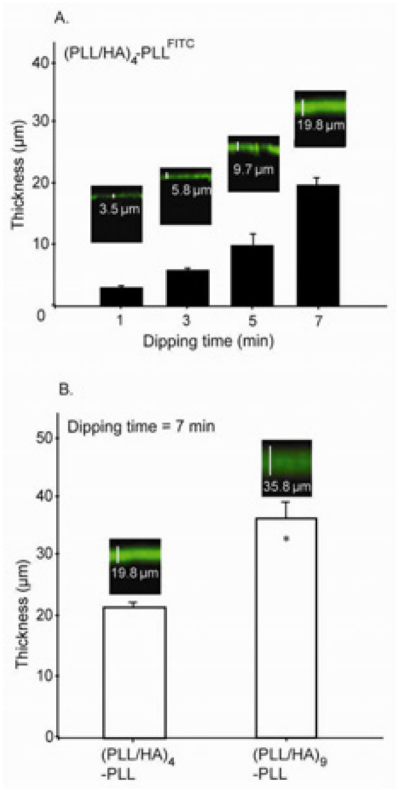

Figure 3.

A. Effect of hydrogel dipping time in polyelectrolyte solution at each deposition step for a $(PLL/HA)_4$-PLL^{FITC} film. The PEM film thickness increased significantly when hydrogel dipping time at each deposition step is increased. **B.** Effect of the number of layer pairs on the film thickness at constant solution-dipping time of 7 min. The PEM-film thickness increased significantly with the number of deposited layer pairs. Inset in A and B shows fluorescence intensity profile images of PLL^{FITC}/HA films built on HA hydrogels in *xz* direction by CLSM (Students t-test, * $p<0.05$).

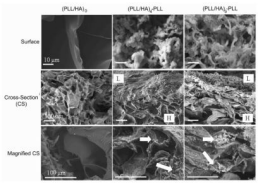

Figure 4.

Environmental scanning electron microscopy images of the top surface and cross-sections of unmodified hydrogels $(HA)_0$ (left column) and hydrogels with $(PLL\text{-}HA)_4$-PLL, and $(PLL\text{-}HA)_9$-PLL films (middle and right columns). The top surface of $(HA)_0$ gel (left images) showed smooth surface whereas both $(PLL\text{-}HA)_4$-PLL (middle images) and $(PLL\text{-}HA)_9$-PLL (right images) showed rough granular/hair-like structure, (maginification 3000X). After multilayer formation, cross-section of hydrogel showed film formation (L) on the top layer in addition to the bottom layer of bulk hydrogel structure (H), (maginification 300X). In bottom row, the modified hydrogels showed diffusion of polyelectrolyte complexes inside the bulk of the hydrogels (marked with white arrow), (maginification 900X).

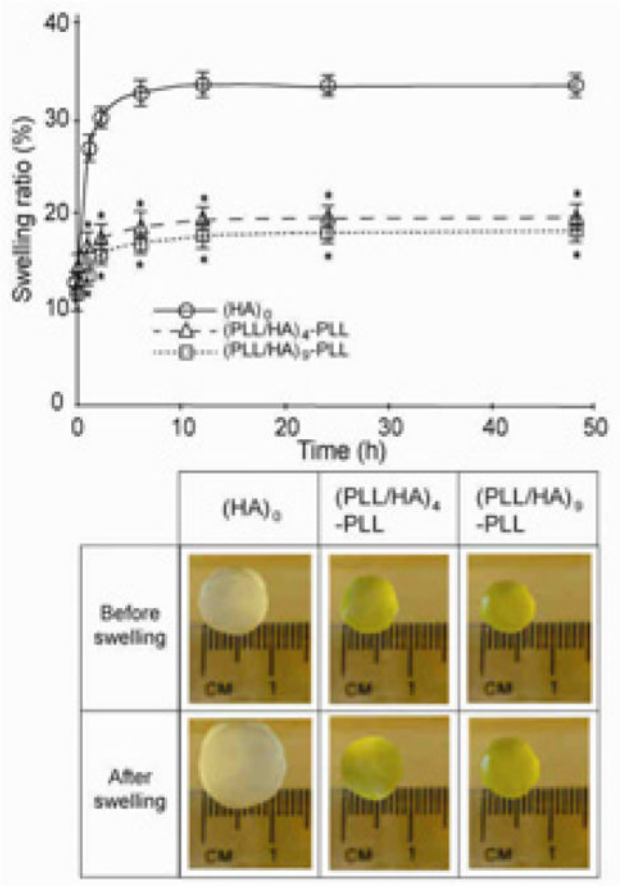

Figure 5.

Effect of PEM film formation on the swelling properties of the hydrogels. **A.** LBL assembly of (PLL^{FITC}/HA) films on HA hydrogels reduced their swelling ratio. Two-way ANOVA revealed a significant effect of the number of layer pairs ($p<0.05$), time in PBS ($p<0.05$) and an interaction between layer number and incubation time in PBS ($p<0.05$) on the swelling ratio of hydrogels. (post-hoc analysis by Fischer's LSD; * $p<0.05$) **B.** Photographs of hydrogels before and after 48h of immersion in PBS.

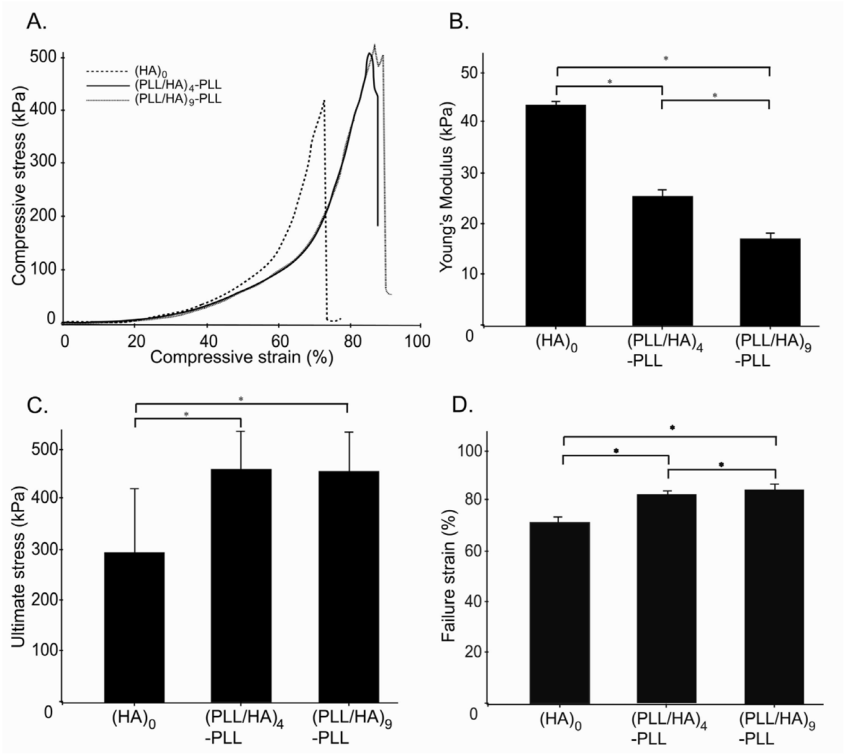

Figure 6.

Mechanical properties of unmodified hydrogels and of PEM-coated hydrogels. **A.** Compressive stress as a function of the strain. **B.** Young's modulus deduced from the linear region of the graph (5–15% strain) in part A. **C.** Ultimate stress **D.** Ultimate strain. (ANOVA followed by Fischer's LSD, * $p<0.05$)

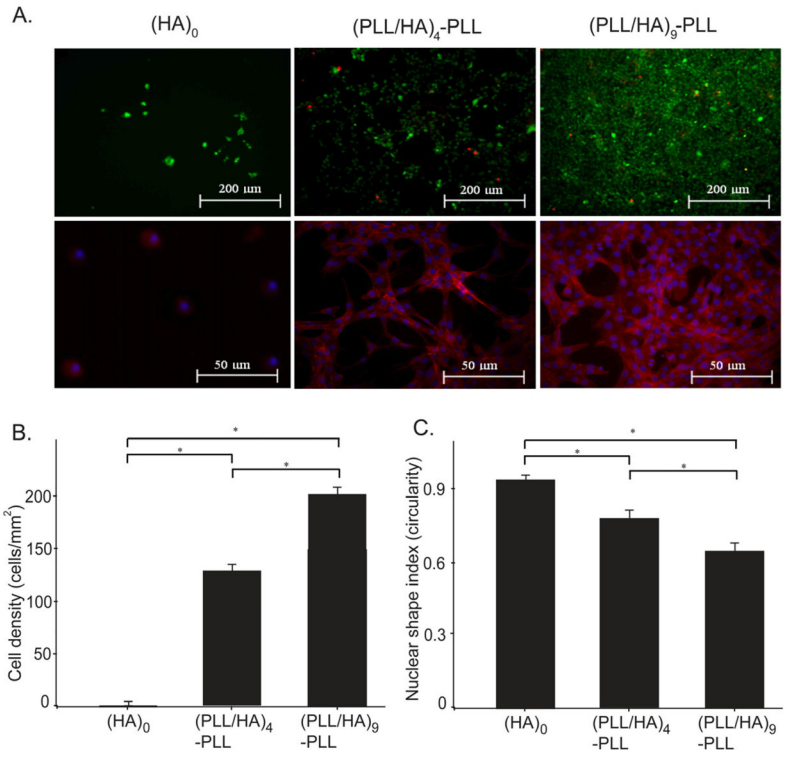

Figure 7.

NIH-3T3 cell adhesion on unmodified hydrogel $(HA)_0$, as well as on PEM-coated hydrogels with $(PLL/HA)_4$-PLL and $(PLL/HA)_9$-PLL films. **A.** Live (green) and dead (red) as well as phalloidin staining images of NIH-3T3 cells 48 h after seeding on the hydrogel surface with and without PEM deposition. High cell viability was evidenced for cells on PEM-coated hydrogels. Phalloidin staining showed the ability of cells to adhere and spread on the hydrogel only after PEM surface modifications. **B.** The addition of layers significantly increased cell density (ANOVA $p<0.05$) as defined as the number of DAPI stained nuclei per hydrogel area. **C.** Layer deposition significantly increased cell spreading (ANOVA, $p<0.05$) as characterized by the shape index; Circularity ($4*\pi*$area/perimeter^2) of each individual cell was evaluated using built-in functions of NIH ImageJ software, with a shape index of 1 representing a circle (ANOVA; Fischer's LSD; * $p<0.01$).